X-690-75-89
PREPRINT

NASA TM X-70873

MODELLING THE MAGNETOSPHERE OF MERCURY

Y. C. WHANG
N. F. NESS

APRIL 1975

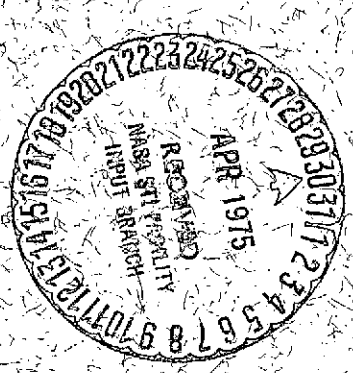

GSFC
GODDARD SPACE FLIGHT CENTER
GREENBELT, MARYLAND

For information concerning availability
of this document contact:

Technical Information Division, Code 250
Goddard Space Flight Center
Greenbelt, Maryland 20771

(Telephone 301-982-4488)

MODELLING THE MAGNETOSPHERE OF MERCURY

by

Y. C. Whang
Department of Aerospace & Atmospheric Sciences
The Catholic University of America
Washington, D. C. 20064

and

N. F. Ness
Laboratory for Extraterrestrial Physics
NASA-Goddard Space Flight Center
Greenbelt, Maryland 20771

April 4, 1975

Submitted to Journal of Geophysical Research

Abstract

A model magnetosphere for Mercury is presented using an upstream image-dipole and nightside 2-dimensional tail current sheet method. The tail field is represented by a new analytical formulation. The magnetic field data from the Mercury I encounter by Mariner 10 in March 1974 are used to determine quantitative parameters of the model magnetosphere, using the method of least squares. The magnetopause crossing points directly observed are used to determine the size of the magnetosphere, and the solar wind conditions are used to determine the magnetospheric field at the stagnation point. The model produces a magnetosphere-like region with planetary field lines that are confined in nearly circular cross-sections transverse to the Sun-planet line. Results are used to show geometry, field line configuration, and contours of constant field intensity inside the magnetosphere.

Introduction

This paper presents a quantitative model of the magnetospheric field of Mercury based on the magnetic field data observed during the first encounter of the Mariner 10 spacecraft with Mercury on 29 March 1974 (hereafter referred to as Mercury I).

The preliminary results from the analysis of the Mercury I data (Ness et al., 1974) unexpectedly revealed that the planet Mercury appeared to have a modest but significant intrinsic magnetic field. The planetary field was compressed and confined by the dynamic pressure of the solar wind plasma to form a magnetosphere-like region. The interaction of the solar wind with Mercury appears Earth-like and includes the formation of a detached bow shock upstream of the planet and magnetic tail downstream. Simultaneous measurements of the low energy electron flux from Mercury I by Ogilvie et al (1974) provided strong correlative evidence for the existence of a planetary magnetosphere and a bow shock. In addition, intense bursts of high energy charged particles were reported on the same spacecraft (Simpson et al. 1974) as occurring in a region of space corresponding to the magnetosphere and magnetosheath. The preliminary analysis of Mercury I data yielding an estimate of the intrinsic planetary field was based on a simple offset tilted dipole model which did not consider external sources of the field.

Important features of the magnetospheric field of Mercury were established in a recent paper by Ness et al. (1975a) in which the field was represented by a set of spherical harmonic functions including external sources. The planet Mercury occupies a very large fraction

of the volume of the magnetosphere since the subsolar point of the magnetopause is only ~0.6 R above the surface of the planet. Thus a substantial part of the observed magnetosphere field, $\vec{B}_{obs}$, is due to external sources and not only the intrinsic field. The final analysis showed that the centered planetary dipole is nearly normal (83^{o}) to the equatorial plane with a polarity sense similar to the Earth's. Significant distortion of the observed magnetospheric field from a dipole field was interpreted as due to the compression by the solar wind and the formation of a magnetic tail. The results suggested that the tail current sheet must be located close to the planet on its dark side.

A second encounter (Mercury II) by Mariner 10 occurred on 21 September 1974. The targeting strategy of the Mercury II mission was to provide optimum imaging coverage of the south polar regions and thus the spacecraft did not approach sufficiently close to the planet to directly observe the magnetospheric field or bow shock of the planet. A third encounter (Mercury III) occurred on 16 March 1975 and additional observations of the magnetospheric field of Mercury were performed which confirmed the existence of an intrinsic field of the planet (Ness et al., 1975b).

Model Magnetosphere

This model study is an attempt to determine some quantitative parameters for the magnetospheric field of Mercury based on Mercury I data. The observed magnetospheric field data available from Mercury I are restricted to a single pass during a time period of 17 minutes. Let F_x, F_y, F_z denote the three components of the observed vector magnetic field in a Mercury-centered solar Ecliptic coordinate system (ME),

where (x,y,z) denote the location of the spacecraft using the planetary radius (R_{μ} = 2439 km) as a unit of length.

Because the available data set is very limited, the model magnetosphere under consideration is a very simple one. As shown in Figure 1, it is justifiably assumed that the intrinsic planetary dipole moment $\vec{M}$, is located at the center of the planet, and is normal to the equatorial plane and the solar wind. Ness et al. (1975a) have determined the orientation of the moment to be $\theta = -80^{\circ}$ and $\phi = 285^{\circ}$ in the ME coordinate system so that the "aspect" angle of solar wind flow relative to the dipole axis is 87.4°, very close to the 90° assumed.

The tail current sheet is assumed to coincide with the equatorial plane on the dark side of Mercury with its edge located at $x = x_t$. We assume that the magnetospheric field is divergent-free and curl-free everywhere except at the tail current sheet and that the field lines are tangential to a magnetosphere-like boundary, i.e. the magnetopause, so that the surface is modeled as a tangential discontinuity.

During the inbound crossing of the magnetopause of Mercury I encounter, the spacecraft was located at

$$x = -1.66$$

and

$$(y^2 + z^2)^{1/2} = 2.30$$

The outbound crossing occurred at

$$x = -0.78$$

and

$$(y^2 + z^2)^{1/2} = 2.30$$

Thus the observed magnetosphere during Mercury I encounter had a radius

of approximately 2.3 between x = -0.8 to -1.7. The stand-off distance to the subsolar point of the magnetopause was not directly observed. However, from the solar wind flow velocity and density measured by the plasma science experiment (Ogilvie et al., 1974), the magnitude of the equivalent magnetic field at the stagnation point to balance the solar wind momentum flux is computed as ≈ 160 gammas.

These conditions will be used in determining quantitative parameters for a model magnetosphere of Mercury. Two different models shall be developed: (1) assumes the magnitude of the planetary dipole moment to be unknown, and (2) constrains the moment to the 5.1×10^{22} Gauss-cm^3 value determined by Ness et al. (1975a). The latter case corresponds to an equatorial field strength of 350γ for the internal dipole.

Tail Field

The tail field is represented by the simple analytical form

$$\left.\begin{aligned} B_x &= -r_t^{-1/2} \sin\tfrac{\omega}{2}\, B_t \\ \text{and} \qquad B_z &= r_t^{-1/2} \cos\tfrac{\omega}{2}\, B_t \end{aligned}\right\} \quad (1)$$

in the region: $r_t > 0$ and $-\pi < \omega < \pi$

Here

$$\left.\begin{aligned} r_t &= \left[(x - x_t)^2 + z^2\right]^{1/2} \\ \text{and} \qquad \omega &= \tan^{-1}\left(\frac{z}{x - x_t}\right) \end{aligned}\right\} \quad (2)$$

where r_t is the distance from the edge of the two-dimensional current sheet. The strength of the tail field is characterized by a constant B_t which represents the magnitude of the tail field at $r_t = 1$. The component $B_y \equiv 0$ since the current sheet extends to infinity in both the + and - y directions.

Equation (1) can be rewritten in the following form as a function

of a complex variable

$$B_z + iB_x = (r_t e^{i\omega})^{1/2} B_t \qquad (3)$$

where B_t is a real constant. This function is single-valued and analytic at all points in the region $r_t > 0$ and $-\pi < \omega < \pi$. Satisfaction of the Cauchy-Riemann conditions shows that the tail field given by (1) is divergent-free and curl-free everywhere except along a branch cut defined by $z = 0$ and $x \leq x_t$ which corresponds to an infinitely thin tail current sheet.

In the absence of other fields, the tail field represented by (1) immediately on each side of the current sheet is parallel to the sheet but in opposite directions on opposite sides. The potential lines are represented by

$$r_t^{1/2} \sin \frac{\omega}{2} = \text{constant}$$

and the magnetic field lines by

$$r_t^{1/2} \cos \frac{\omega}{2} = \text{constant}$$

Figure 2 shows the geometry of magnetic field lines of the tail current sheet.

Magnetospheric Field

The image-dipole method (Hones, 1963; Taylor and Hones, 1965) is used to represent the contribution to the magnetospheric field of Mercury from the electrical currents associated with the deflected solar wind flow, which forms the magnetopause. Let

$$\vec{M} = g_1^0 \vec{e}_z$$

denote the moment of the centered planetary dipole. An image dipole

with a moment of

$$\vec{M}_i = \Gamma \vec{M}$$

is placed at $(x_i, 0, 0)$, in the sunward direction. The image dipole represents the effects of confining the planetary field within a magnetopause. Adding the tail field (1) to the field due to $\vec{M}$ and $\vec{M}_i$, we write the net field vector for the model magnetosphere of Mercury as

$$\vec{B}_{model} = -g_1^0(c_{11}\vec{e}_x + c_{21}\vec{e}_y + c_{31}\vec{e}_z) + B_t(c_{12}\vec{e}_x + c_{32}\vec{e}_z) \qquad (6)$$

where

$$c_{11} = -3z\left(\frac{x}{r^5} + \frac{x - x_i}{r_i^5}\Gamma\right)$$

$$c_{21} = -3zy\left(\frac{1}{r^5} + \frac{\Gamma}{r_i^5}\right)$$

$$c_{31} = \frac{1}{r^3}\left(1 - \frac{3z^2}{r^2}\right) + \frac{\Gamma}{r_i^3}\left(1 - \frac{3z^2}{r_i^2}\right)$$

$$c_{12} = -r_t^{-1/2}\sin\frac{\omega}{2}$$

$$c_{32} = r_t^{-1/2}\cos\frac{\omega}{2}$$

Here r denotes the distance from the center of Mercury, and r_i the distance from the image dipole. The model field (6) is tangential to a boundary surface which corresponds to the magnetopause, and it is divergent-free and curl-free everywhere within the magnetosphere except at the tail current sheet.

Method of Least Squares

For a given set of N data points, the vector field residual, or mean squared deviation between theory and observation can be written as

$$\sigma^2 = \frac{1}{N-1} \sum_{n=1}^{N} (\vec{B}_{model} - \vec{B}_{obs})^2 \qquad (7)$$

$$= \frac{1}{N-1} \sum_{n=1}^{N} \left[(c_{11} g_1^o + c_{12} B_t - F_x)^2 + (c_{21} g_1^o - F_y)^2 + (c_{31} g_1^o + c_{32} B_t - F_z)^2 \right]$$

σ^2 is controlled by five parameters: g_1^o, B_t, Γ, x_i and x_t. The minimum of σ^2 is the best fit to the data and is determined by setting $\frac{\partial \sigma^2}{\partial g_1^o} = 0$ and $\frac{\partial \sigma^2}{\partial B_t} = 0$. Thus, a system of two normal equations results:

$$b_{i1} g_1^o + b_{i2} B_t = b_{i3} \qquad (i = 1,2) \qquad (8)$$

where

$$b_{11} = \sum_{n=1}^{N} (c_{11}^2 + c_{21}^2 + c_{31}^2)$$

$$b_{12} = b_{21} = \sum_{n=1}^{N} (c_{11} c_{12} + c_{31} c_{32})$$

$$b_{13} = \sum_{n=1}^{N} (c_{11} F_x + c_{21} F_y + c_{31} F_z)$$

$$b_{22} = \sum_{n=1}^{N} (c_{12}^2 + c_{32}^2)$$

$$b_{23} = \sum_{n=1}^{N} (c_{12} F_x + c_{32} F_z)$$

Making use of (7) and (8), for any given set of N data, B_t, g_1^o, (if necessary), and σ^2 as functions of the three model parameters Γ, x_i, and x_t can be calculated.

The best fit model magnetosphere is thus governed by these three parameters: Γ, the ratio of the moment of the image dipole to that of

Mercury's dipole, x_i the distance between the two dipoles and x_t the position for the edge of the tail current sheet. It is necessary to adjust these three parameters until a best-fit model magnetosphere is obtained. The geometry of the magnetopause is mainly controlled by Γ and x_i. For any given pair of Γ and x_i, the value of x_t is adjusted until a minimum value of σ^2 is obtained.

Magnetosphere with Unknown Planetary Dipole Moment (Model 1)

The Mercury I magnetic field data during the intervals from 2038 to 2047 UT and from 2049 to 2052 UT (Ness et al, 1975a) have been used to construct a representative magnetospheric field of Mercury. When the spacecraft was inside the magnetosphere of Mercury, abrupt increases in the flux of charged particles have been observed (Simpson et al. 1974). Inside the magnetosphere this observed feature at ~2048 UT was designated as the B event and that at ~2053 UT as the C event. (The D event occurred outside the magnetosphere and the A event was quite small in comparison). Magnetic field data during the B and C events are not used in this study.

To meet the condition that the net magnetospheric field is approximately 160 gammas at the stagnation point, a series of possible solutions was found which corresponded to a varying value of Γ. The size of the magnetosphere increases as the dipole ratio Γ decreases. The geometry of the magnetosphere that best-fits the magnetopause crossing points directly observed during Mercury I for the case of g_1^o variable has a value of σ = 16.5 gammas. At the radial distance to the sub-solar point of the magnetopause, x_{stag} = 1.33, the dipole field is "amplified" by a factor of 2.35. A comparison of the model magnetospheric field with the observed field is shown in Figure 3. The value of g_1^o gives a

dipole moment of the intrinsic field = 2.3×10^{22} Gauss-cm^3, which is approximately one half that obtained from the earlier studies. The other pertinent parameters are $x_i = 6.44$, $\Gamma = 93.5$, $x_t = -1.5$ and $B_t = -35.1$ gammas.

Figure 4a shows the geometry of the model magnetopause and the field lines within the magnetosphere. The cross-sections of the magnetopause on planes normal to the Sun-Mercury line are nearly circular. Their radius near x = -1 is approximately 2.3 which is in good agreement with the observed crossing points of the magnetopause.

Figure 5a shows the iso-intensity field contours of the model magnetosphere in the noon-midnight meridian plane. The presence of the tail current sheet introduces a neutral line just forward of the sheet on the equatorial plane. The singularity line along the edge of the sheet is a mathematical construct due to the assumed infinitely thin tail current sheet in this model.

Magnetosphere with Known Planetary Dipole Moment (Model 2)

In case the planetary dipole moment is known, the method of least squares leads to a single normal equation which determines the characteristic magnitude of the tail field

$$B_t = (b_{23} + b_{21} g_1^o) b_{22} \qquad (9)$$

Assuming that $g_1^o = -350$ gammas for Mercury, the same set of Mercury I magnetic field data is used to study another model of the magnetosphere of Mercury. To meet the condition that the magnetospheric field is approximately 160 gammas at the stagnation point, a series of possible solutions corresponding to a varying value of Γ is again obtained. Model magnetospheres determined by this series of solutions have

σ-values always greater than 37 gammas. Figure 4b shows the geometry of the magnetopause and field lines in the noon-midnight meridian plane represented by a model with fixed g_1^o =-350 gammas. Figure 5b presents the corresponding iso-intensity field contours in the noon-midnight meridian plane. In this case, the stagnation point distance is found to be 1.71 with a tail field B_t = -91.6γ and x_t = -1.95 while the image dipole is located at x_i = 10.4 with a strength Γ = 264 which combine to yield σ = 46γ. The fit to observations is shown in Figure 3.

Discussion

Quantitative models of the magnetosphere of Mercury have been developed which are useful in studying the interaction of the solar wind with Mercury and the magnetic field geometry within the magnetosphere. When the momentum flux of the solar wind changes, the stand-off distance and the magnetospheric field at the stagnation point varies. The present models predict that the stand-off distance will vary between 1.2 and 1.7 under varying solar wind conditions and that theoretically it is very unlikely that the solar wind can directly impact the surface of Mercury except via access at neutral points in the polar regions. This problem has also recently been studied empirically by Siscoe and Christopher (1975), who reached the same conclusion using solar wind measurements at 1 AU, scaled to the orbit of Mercury, i.e. between 0.31 - 0.47 AU.

The present model will be best suited for study of the magnetospheric field near the noon-midnight meridian plane and will be less valuable when approaching the downstream flanks. This is due to the use of a 2 dimensional tail current sheet, rather than a restricted

3 dimensional tail current sheet. Constraining the dipole term leads to a substantially inferior fit to the observed data at Mercury I. Although the direction of the field is moderately close, the magnitude is consistently larger than actually observed.

The observations at Mercury III will help in ascertaining which of the two models, and hence g_1^o values, are closer to the actual case. It may also be expected that relaxing the condition that the observed magnetopause crossings agree well with the theoretical model will yield a more realistic field configuration in the region near the noon-midnight meridian plane, $|y| < 1.5$. This will be especially true if the stagnation point distance is predetermined by a scaling from an analogy with the terrestrial magnetosphere.

In either of the models, there is little if any indication of the development of a field configuration which could confine charged particles in a "trapped" or radiation belt structure. This is because of the large day-night asymmetrices of the field associated with its significant compression by the solar wind on the dayside and extension on the nightside to form a magnetic tail. The magnetospheric field is so distorted that a careful study of an accurate model shall be required to further quantify these remarks. There are large spatial gradients of the magnetic field intensity so that slight changes in the solar wind momentum flux and direction, may lead to significant changes in the comparisons with actual observations. A more accurate model would then begin by using a solar magnetospheric coordinate system to account for the 10^o obliquity of the dipole axis to the ecliptic and a 3 dimensional confined tail current sheet.

Acknowledgements

We thank K. W. Behannon and R. P. Lepping for many useful discussions and their important contributions to the magnetic field experiment. The work at The Catholic University of America was supported by the National Aeronautics and Space Administration under grant NGR-09-005-063.

References

Hones, E. W., Jr., Motions of changed particles trapped in the Earth's magnetosphere, J. Geophys. Res., 68, 1209, 1963.

Ness, N. F., K. W. Behannon, R. P. Lepping, Y. C. Whang and K. W. Schatten, Magnetic field observations near Mercury: Preliminary results from Mariner 10, Science, 185, 151, 1974.

Ness, N. F., K. W. Behannon, R. P. Lepping and Y. C. Whang, The magnetic field of Mercury: Part I, J. Geophys. Res., ___, (in press) 1975a.

Ness, N. F., K. W. Behannon, R. P. Lepping and Y. C. Whang, Magnetic field of Mercury Confirmed, Nature, in press, 1975b.

Ogilvie, K. W., J. D. Scudder, R. E. Hartle, G. L. Siscoe, H. S. Bridge, A. J. Lazarus, J. R. Asbridge, S. J. Bame, and C. M. Yeates, Observations at Mercury encounter by the plasma science experiment on Mariner 10, Science, 185, 145, 1974.

Simpson, J. A., J. H. Eraker, J. E. Lamport, and P. H. Walpole, Electrons and protons accelerated in Mercury's magnetic field, Science, 185, 160, 1974.

Siscoe, G. L. and L. Christopher, Variations in the Solar Wind Stand-off Distance at Mercury, Geophys. Res. Letters, in press, 1975.

Taylor, H. E., and Hones, E. W., Jr., Adiabatic motion of auroral particles in a model of the electric and magnetic fields surrounding the Earth, J. Geophys. Res., 70, 3605, 1965.

Figure Captions

Figure 1 A model magnetosphere of Mercury includes a tail current sheet coincide with the equatorial plane on the darkside of the planet. The tail current sheet has a straight edge located at $x = x_t$.

Figure 2 The field line topology of the 2 dimensional tail field.

Figure 3 The field intensity F, latitude θ and longitude ϕ of the model magnetospheres compared with observed data along the trajectory of Mercury I.

Figure 4 Field lines and magnetopause shapes in the noon-midnight meridian plane of the model magnetospheres of Mercury.

Figure 5 Field iso-intensity contours in the model magnetospheres in the noon-midnight meridian plane.

MODEL MAGNETOSPHERE OF MERCURY

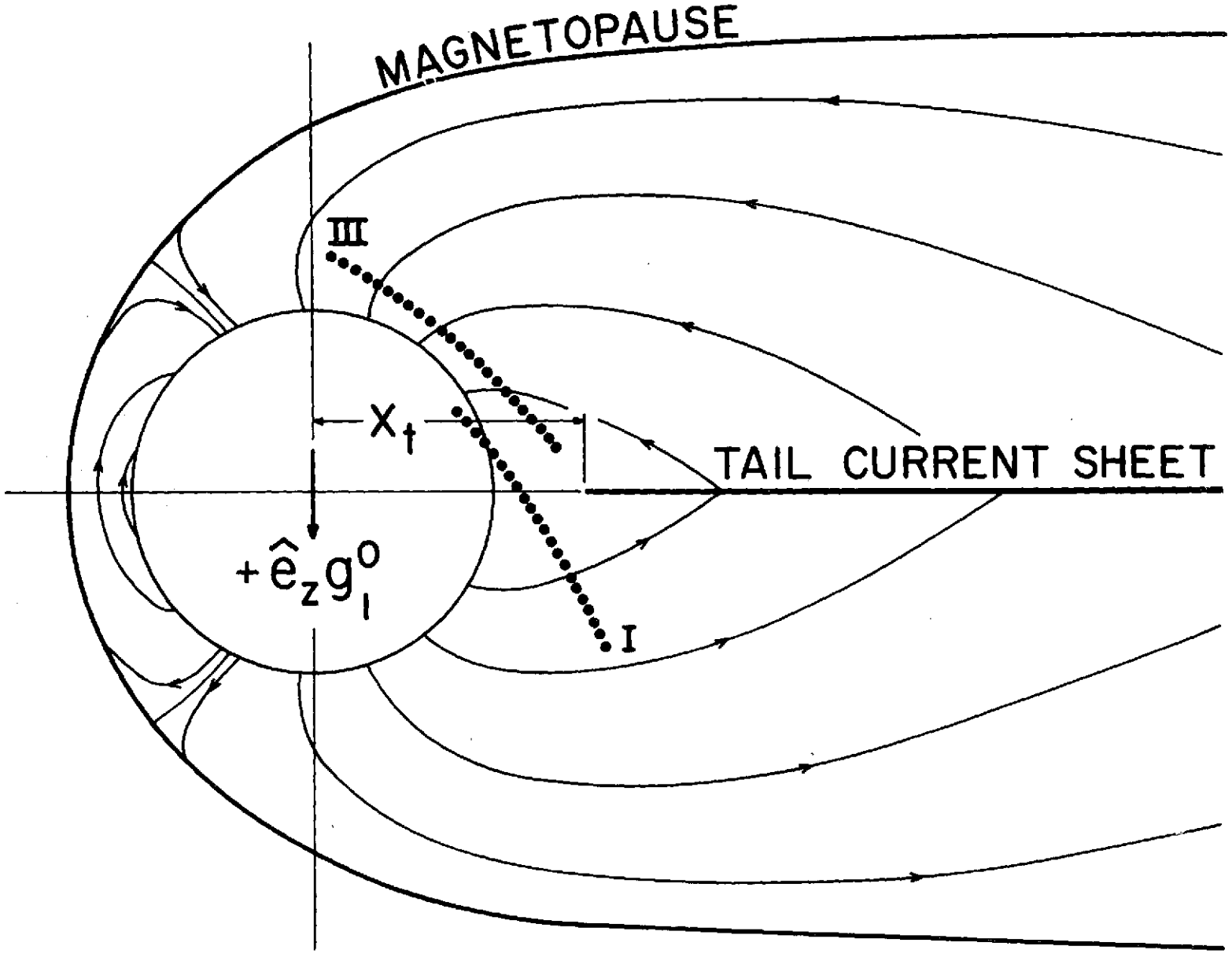

Figure 1

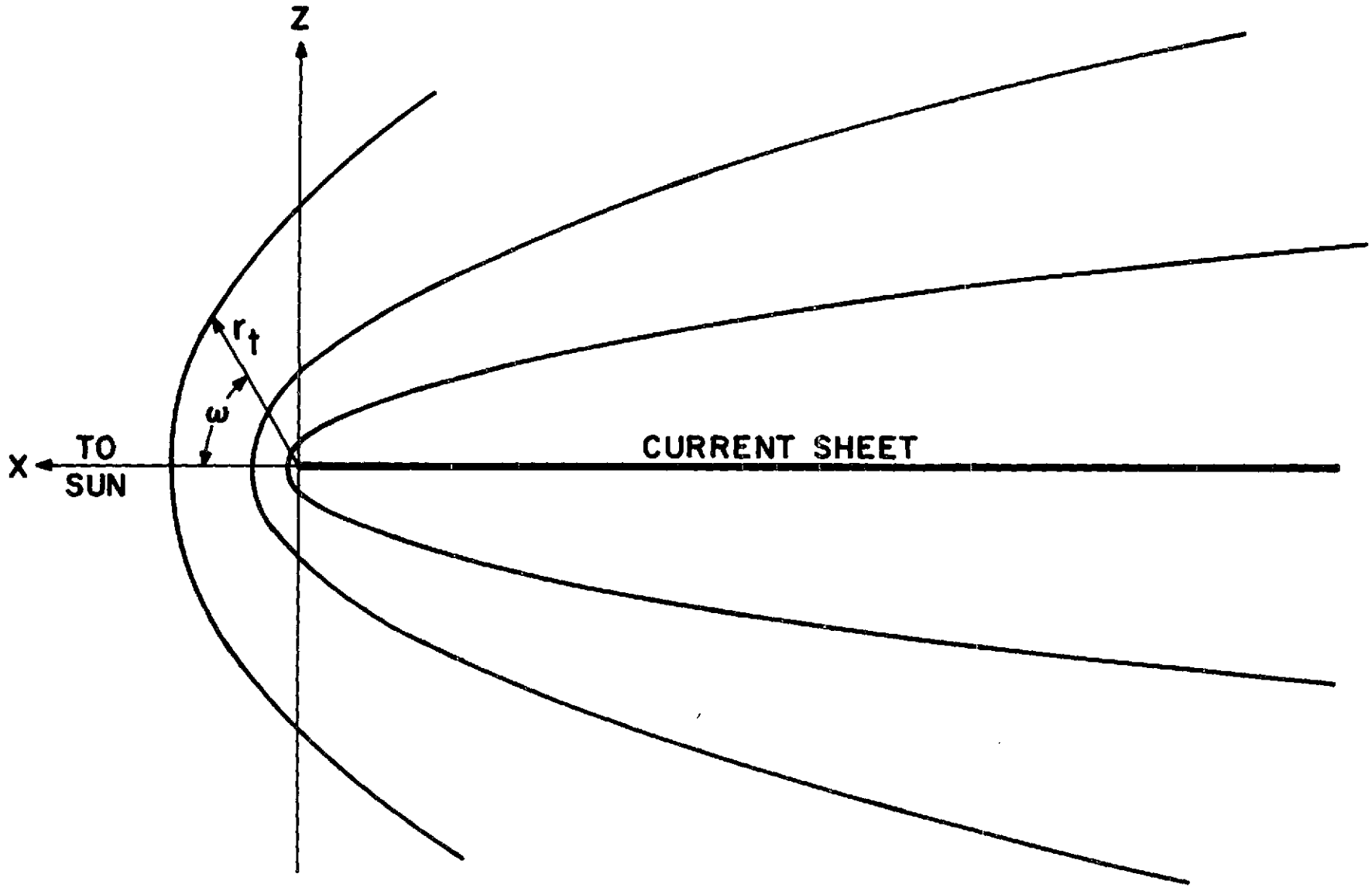

FIELD LINES OF MODEL TAIL CURRENT

Figure 2

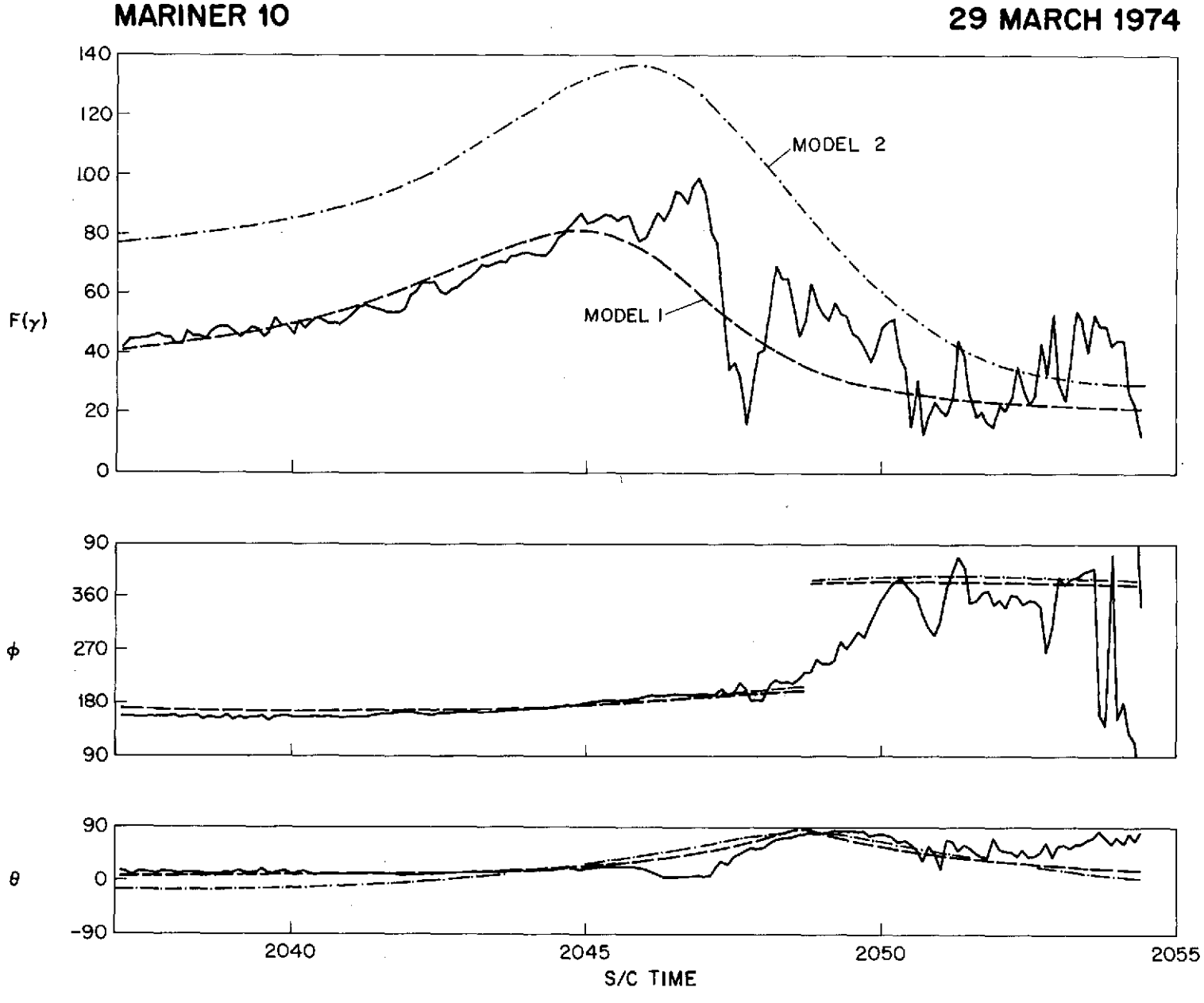
MARINER 10
29 MARCH 1974
140
120
100
80
60
40
20
0
F(γ)
MODEL 2
MODEL 1
90
360
270
180
90
ϕ
90
0
-90
θ
2040
2045
2050
2055
S/C TIME

Figure 3

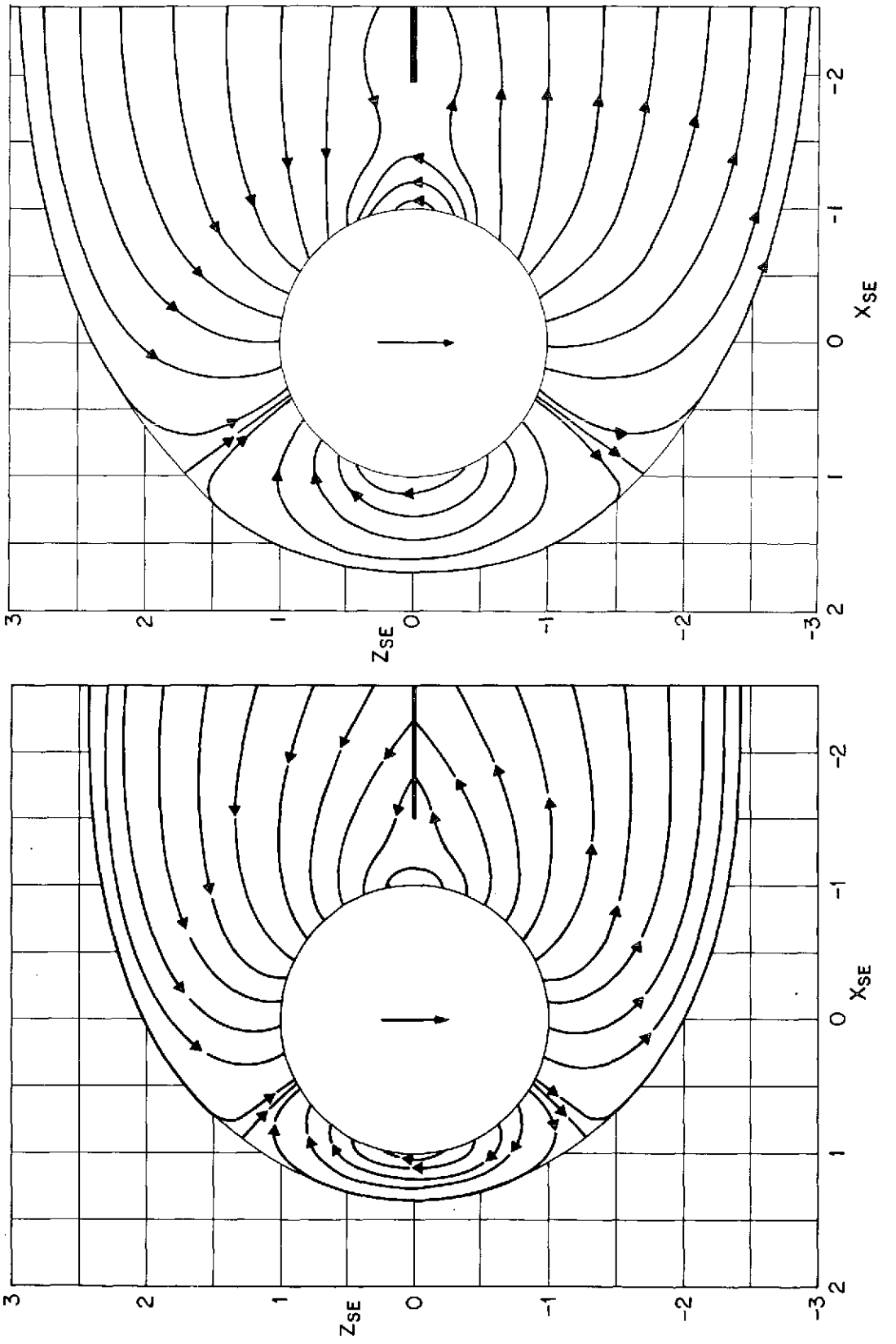

Figure 4

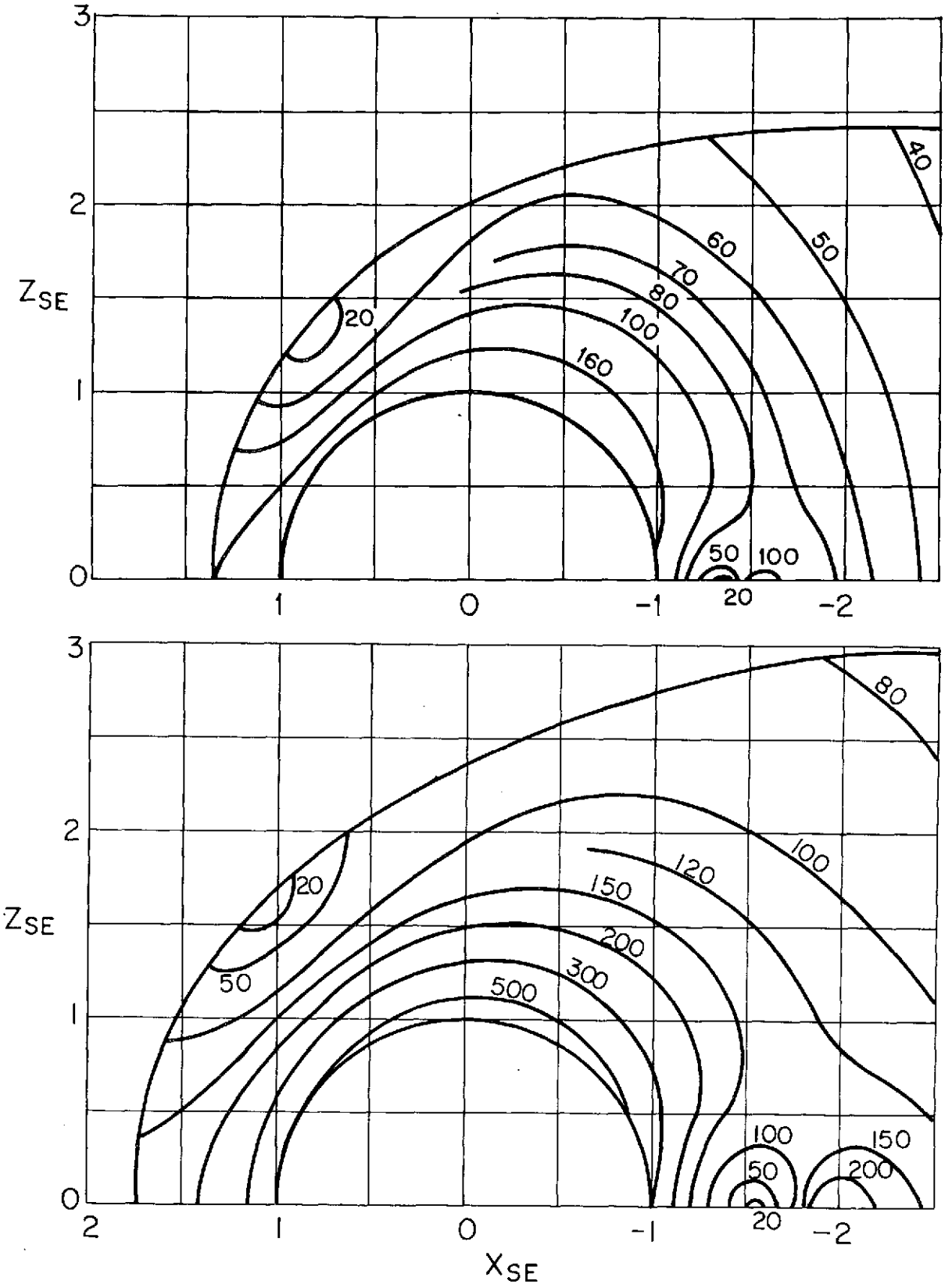
3
2
1
0
Z_{SE}
40
50
60
70
80
100
160
20
50
100
20
1
0
-1
-2
3
2
1
0
Z_{SE}
80
100
120
150
200
300
500
20
50
100
150
200
50
20
2
1
0
-1
-2
X_{SE}

Figure 5